JOURNAL OF SOLID STATE CHEMISTRY 91, 121–125 (1991)

The Growth and Single Crystal Structure of a High Pressure Phase of Molybdenum Trioxide: MoO_3-II*

E. M. McCARRON III AND J. C. CALABRESE

Central Research and Development Department, E. I. du Pont de Nemours and Company, Experimental Station, Wilmington, Delaware 19880-0356

Received July 31, 1990; in revised form November 1, 1990

Single crystals of a new high pressure modification of molybdenum trioxide, MoO_3-II, were grown in a tetrahedral anvil apparatus at elevated temperature. The structure of MoO_3-II is monoclinic, $P2_1/m$, with unit cell parameters: a = 3.954(1) Å, b = 3.687(2) Å, c = 7.095(4) Å, and β = 103.75(4)°. MoO_3-II (4.75 g/cm^3) is metastable at ambient pressure and converts to less dense orthorhombic α-MoO_3 (4.71 g/cc) rapidly at temperatures above ~200°C. Like the α-MoO_3 structure, the structure of MoO_3-II is layered. In fact, the individual $MoO_{3/3}O_{2/2}O_{1/1}$ layers of the two phases are virtually identical. However, the stacking sequence of the layers of MoO_3-II (*aaa*) differs from that of α-MoO_3 (*aba*). This is equated with an improved packing efficiency for the layers of MoO_3-II versus those of α-MoO_3.

Introduction

In addition to the thermodynamically stable α-MoO_3 phase, two metastable polymorphs of molybdenum trioxide have been discovered recently, namely, β-MoO_3 (*1, 2, 3*) and β'-MoO_3 (*4*). Briefly, α-$MoO_{3/3}O_{2/2}O_{1/1}$ has a unique 2D layered structure (*5*), whereas, β- and β'-$MoO_{6/2}$ are related to the 3D ReO_3 structure. Studies (*6*) of the correlation between the α- and β-MoO_3 structure-types and catalytic activity, in particular, with regard to the selective oxidation of methanol to formaldehyde (*7*), prompted a search for the existence of other MoO_3 phases. It was hypothesized that the layered structure of α-MoO_3 might collapse at high pressure to form a more condensed phase. This was not observed. Recently Åsbrink *et al.* (*8*) studied the lattice parameters of α-MoO_3 as a function of pressure at ambient temperature and also observed no new MoO_3 structure-types. However, we find that the combination of high pressure *and high temperature* does indeed result in the formation of a new phase, MoO_3-II. In this paper, we describe the single crystal structure and properties of MoO_3-II in detail and compare the structure to that of α-MoO_3.

Experimental

Powder samples of MoO_3-II were prepared routinely from α-MoO_3 (Johnson Matthey Chemicals—Puratronic) in a tetrahe-

* Contribution No. 5608.

0022-4596/91 $3.00

dral anvil apparatus (gold sample container) at 60 kbar and 700°C. Powder samples prepared in this way appeared white with a slightly greenish tint. Single crystals of MoO_3-II were prepared in the same apparatus at 65 kbar with the following heat treatment: hold 15 hr at 1000°C; slow cool at 20°C/hr to 760°C; and furnace cool to room temperature. Crystals prepared in this manner appeared darker than the powder samples above, suggesting that some amount of reduction had occurred. However, powder patterns (Table I) taken from ground single crystals were indistinguishable from those of the white MoO_3-II powder.

TABLE I

POWDER PATTERN OF MoO_3-II

h	k	l	$2\theta^a$	d (Å)	I (calc)^b	I (obs)^b
0	0	1	12.85	6.8917	292.6	43
1	0	0	23.16	3.8407	186.8	23
1	0	−1	23.69	3.7559	698.2	90
0	0	2	25.86	3.4458	352.9	100
0	1	1	27.43	3.2510	1000.0	82
1	0	1	29.18	3.0598	190.9	18
1	0	−2	30.46	2.9349	1.3	—
1	1	0	33.70	2.6598	418.2	31
1	1	−1	34.07	2.6311	21.8	6
0	1	2	35.66	2.5175	75.4	1
1	1	1	38.22	2.3546	20.9	5
1	0	2	39.05	2.3068	78.8	sh
0	0	3	39.22	2.2972	225.0	100
1	1	−2	39.23	2.2962	95.8	
1	0	−3	40.69	2.2173	81.2	14
2	0	−1	45.94	1.9752	131.3	36
1	1	2	46.43	1.9556	64.4	26
0	1	3	46.58	1.9497	80.7	
2	0	0	47.34	1.9203	26.8	7
1	1	−3	47.87	1.9001	14.3	4
2	0	−2	48.47	1.8780	81.9	20
0	2	0	49.44	1.8435	180.4	24
1	0	3	50.94	1.7927	0.1	—
0	2	1	51.30	1.7809	15.2	5
2	0	1	52.41	1.7457	61.4	13
2	1	−1	52.56	1.7411	89.4	20
1	0	−4	52.81	1.7334	44.0	21
0	0	4	53.16	1.7229	3.6	sh
2	1	0	53.82	1.7032	107.1	16
2	0	−3	54.51	1.6833	0.7	—
2	1	−2	54.86	1.6734	26.4	7
1	2	0	55.27	1.6620	30.7	8
1	2	−1	55.53	1.6549	121.6	16
0	2	2	56.62	1.6255	74.3	14
1	1	3	57.13	1.6122	103.6	15
1	2	1	58.45	1.5791	49.5	11
2	1	1	58.50	1.5778	16.0	sh
1	1	−4	58.87	1.5687	57.4	
1	2	−2	59.18	1.5611	0.4	37
0	1	4	59.19	1.5609	132.4	

[a] Copper radiation; λ = 1.54180 Å.

[b] Strong preferred orientation (associated with the layer stacking axis) is observed for both MoO_3-II and α-MoO_3; sh = shoulder.

Crystal Structure Determination

Data were collected with an Enraf-Nonius CAD4 X-ray diffractometer equipped with a monochromatic MoK_α source using a parallelepiped crystal of MoO_3-II with dimensions (0.03 × 0.03 × 0.07 mm). Fourteen diffraction maxima were located and used to obtain cell parameters with dimensions a = 3.954(1) Å, b = 3.687(2) Å, c = 7.095(4) Å, and β = 103.75(4)°. For Z = 2, the calculated density is 4.754 g/cm^3.

A total of 462 reflections was collected at room temperature using the ω-scan mode in the range, 5.9° < 2θ < 49.9°, with a 2.30–2.50° scan width and a 2.00°/min fixed scan speed. There was no evidence of radiation damage to the crystal during data collection. The data were treated in the usual fashion for Lorentz-polarization and absorption (DIFABS (*9*)), yielding 198 unique reflections with $I > 2.0\,\sigma$. Transmission factors varied from 0.59 to 1.59.

The structure was solved[1] using an automated Patterson solution method which required that the molybdenum and three independent oxygen atoms lie on the mirror plane. The model was refined in space group $P2_1/m$ (No. 11) with full matrix least squares

[1] Crystallographic calculations were performed on a DEC/CRAY computer network, using a system of programs developed by J. C. Calabrese. The package incorporates the DIFABS absorption method (*9*) and the ORTEP plot program (*10*).

TABLE II

FRACTIONAL COORDINATES (×10,000) AND ISOTROPIC THERMAL PARAMETERS FOR MoO_3-II

Atom	x	y	z	B_{iso}
Mo	3286 (4)	2500	2966 (2)	0.5 (1)
O(1)	4401 (31)	−2500	3691 (19)	0.5 (3)
O(2)	−924 (29)	2500	3240 (18)	0.5 (3)
O(3)	2709 (35)	2500	547 (20)	1.3 (4)

TABLE III

ANISOTROPIC THERMAL PARAMETERS (Å × 1000)
$\exp[-19.739(U_{11}hha^*a^*... + 2(U_{12}hka^*b^*...))]$

Atom	U_{11}	U_{22}	U_{33}	U_{12}	U_{13}	U_{23}
Mo	6.7 (8)	6.3 (9)	5.2 (9)	0.0	0.9 (6)	0.0
O(1)	8 (6)	2 (7)	13 (7)	0	7 (5)	0
O(2)	4 (6)	1 (6)	11 (6)	0	−2 (5)	0
O(3)	18 (7)	17 (8)	15 (7)	0	10 (6)	0

to $R = 0.048$ and $R_w = 0.061$, where $R_w = [\Sigma w(|F_0| - |F_c|)^2/\Sigma w(|F_0|^2]$ with $\omega \propto [\sigma^2(I) + 0.0009(I)^2]^{-1/2}$. The final e.s.d. of an observation of unit weight is 2.60. The largest final difference-Fourier residual was 1.79 e/Å^3 near the molybdenum atom. Atomic scattering factors were taken from the "International Tables for X-ray Crystallography."

Tables II and III list the final positional parameters and the anisotropic thermal parameters for MoO_3-II, respectively. Bond lengths and angles are given in Table IV.

Discussion

Figure 1 concisely illustrates the major structural difference between the layered phases, MoO_3-II and α-MoO_3. While the individual layers of each phase are nearly identical (see below), a change in the stacking sequence from *aaa* for high pressure MoO_3-II to *aba* for ambient pressure α-MoO_3 occurs, such that, the following relationships exist:

	MoO_3-II monoclinic			α-MoO_3 orthorhombic	
	a	(3.954 Å)	≈	a	(3.963 Å);
	b	(3.687 Å)	≈	c	(3.696 Å);
and	$c \sin \beta$	(6.892 Å)	≈	$b/2$	(6.928 Å).

Conversion of α-MoO_3 to MoO_3-II involves displacements of the molybdenum and oxygen atoms of the b layer of the α-MoO_3 structure, relative to the a layer, which are equivalent to a 180° rotation of the b layer about the stacking axis (Fig. 1). As noted in this study and elsewhere (*8*), high pressure alone is insufficient to bring about this phase change. The necessity for high temperature in addition to high pressure is most likely the result of a small driving force associated with the α-MoO_3 to MoO_3-II phase transformation—the relative density increase being ~1% (4.71 g/ml vs 4.75 g/cm^3, respectively). The major com-

TABLE IV

A COMPARISON OF BOND LENGTHS (Å) AND BOND ANGLES (°) IN MoO_3-II AND α-MoO_3[a]

Bond Lengths	MoO_3-II	α-MoO_3
Mo–O(1)a	2.331 (13)	2.332
Mo–O(1) (2×)	1.937 (4)	1.948
Mo–O(2)b	2.251 (11)	2.251
Mo–O(2)	1.721 (11)	1.734
Mo–O(3)	1.677 (14)	1.671
$O(3)_{mp}$–$O(3)_{mp}$[b]	0.754	0.793
Bond Angles	**MoO_3-II**	**α-MoO_3**
O(1)–Mo–O(1)	144.3 (7)	143.1
O(2)–Mo–O(2)b	168.9 (7)	167.8
O(3)–Mo–O(1)a	165.2 (4)	164.9

[a] Symmetry operation codes:

a	$1 - x$,	$1/2 + y$,	$1 - z$;
b	$1 + x$,	y,	z.

[b] $O(3)_{mp}$–$O(3)_{mp}$ represents the distance between the *m*ean *p*lanes of adjacent O(3) oxygens in adjacent layers.

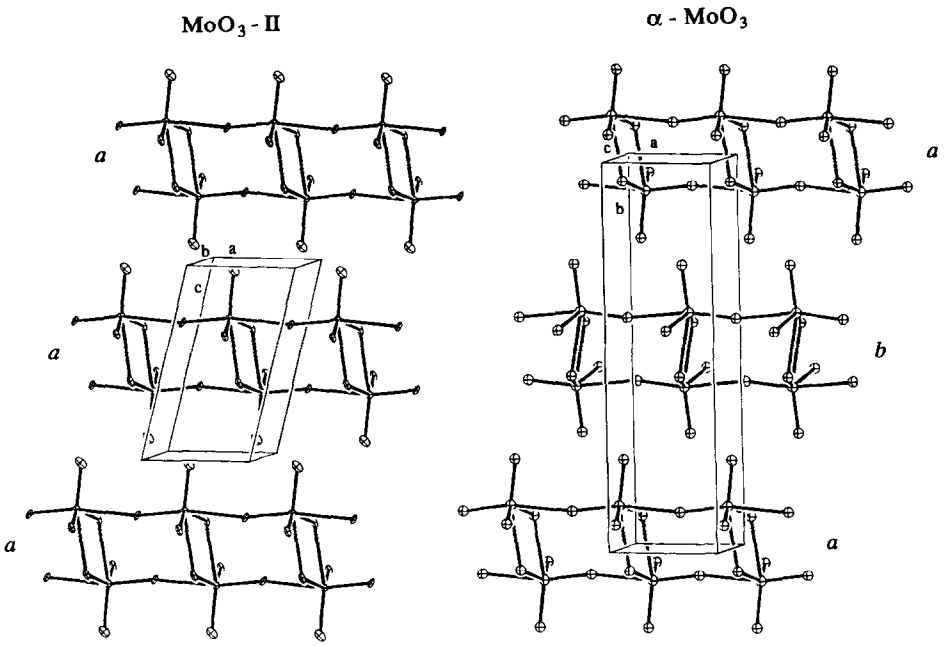

FIG. 1. The structures of MoO_3-II and α-MoO_3 with emphasis on the change in layer stacking.

ponent of this density increase is the compression of the structure along the layer stacking axis (a factor of 4 greater than either orthogonal axis). For reasons discussed below, this compression equates with an increased interpenetration of the molybdenyl oxygens in the Van der Waals gap (as measured by the $O(3)_{mp}$–$O(3)_{mp}$ distance; Table IV). Therefore, the packing of the layers of MoO_3-II is seen as being more efficient than that of α-MoO_3.

Figure 2 and Table IV compare the basic

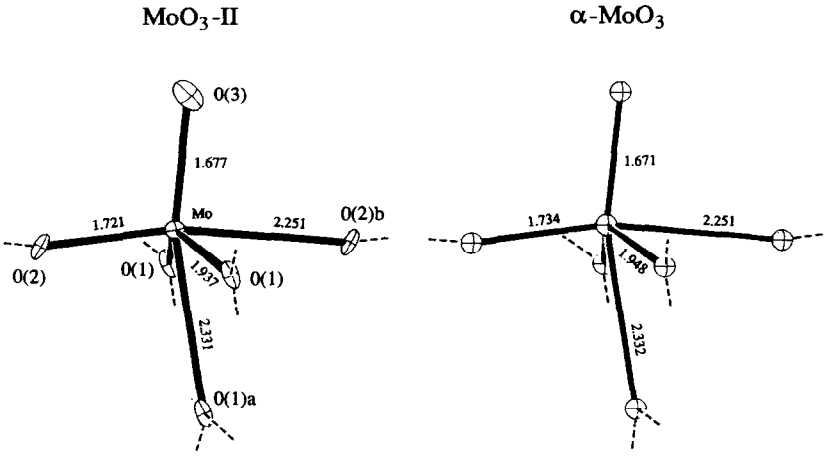

FIG. 2. Equivalent views of the $MoO_{3/3}O_{2/2}O_{1/1}$ octahedra of MoO_3-II and α-MoO_3 (bond lengths in Å)

$MoO_{3/3}O_{2/2}O_{1/1}$ building blocks of both the high and the low pressure forms of molybdenum trioxide. It is interesting to note that in his description of the molybdenum trioxide structure, Kihlborg (*5*) depicted α-MoO_3 as being comprised of infinite chains of $MoO_{2/2}O_{2/1}$ tetrahedra, with only weak interchain interactions (through the Mo–O bonds equivalent to the Mo–O(1)a and Mo–O(2)b bonds of the MoO_3-II structure) resulting in the formation of the unique MoO_3 double layer (Fig. 1). If this structural interpretation is correct, then one might predict that, upon high pressure phase transformation, these long interchain bond distances would be unaffected, since any compression along these bonds would necessitate a corresponding lengthening of the shorter intrachain bonds in order to maintain bond order, i.e., the coordination would more closely approach octahedral. Within statistical limits, the molybdenum coordination spheres of MoO_3-II and α-MoO_3 are virtually the same (Fig. 2). In light of this observation, the structural description of MoO_3 by Kihlborg (*5*), namely, that the structure can be viewed as being built up of weakly interacting tetrahedral chains, is further supported.

Acknowledgments

The authors greatly appreciate the efforts of the powder X-ray diffraction group, in particular, C. Foris (for Guinier diffraction data), G. Jones (for temperature programmed diffraction data), and R. Wroten and R. L. Harlow I (in obtaining the drawings). The technical assistance of M. Sweeten is also appreciated.

References

1. E. M. McCarron, III, *J. Chem. Soc. Chem. Commun.* **1986,** 336.
2. F. Harb, B. Gerand, G. Nowogrocki, and M. Figlarz, *C. R. Acad. Sci. Paris Ser. II* **303,** 349 (1986).
3. G. Svensson and L. Kihlborg, *React. Solids* **3,** 33 (1987).
4. J. B. Parise, E. M. McCarron III, and A. W. Sleight, *Mater. Res. Bull.* **22,** 803 (1987).
5. L. Kihlborg, *Arkiv Kemi* **21,** 357 (1963) and references therein.
6. W. E. Farneth, E. M. McCarron III, A. W. Sleight, and R. H. Staley, *Langmuir* **3,** 217 (1987).
7. For a review see: E. M. McCarron III and A. W. Sleight, *Polyhedron* **5,** 129 (1986).
8. S. Åsbrink, L. Kihlborg, and M. Malinkowski, *J. Appl. Crystallogr.* **21,** 960 (1988).
9. N. Walker and D. Stuart, *Acta Crystallogr.* **A39,** 158 (1983).
10. C. K. Johnson, 1971.